energies

MDPI

Article

Experimental and Theoretical Investigation of the Natural Convection Heat Transfer Coefficient in Phase Change Material (PCM) Based Fin-and-Tube Heat Exchanger

Saulius Pakalka [1,2], Kęstutis Valančius [1] and Giedrė Streckienė [1,*]

[1] Department of Building Energetics, Vilnius Gediminas Technical University, Sauletekio ave. 11, 10223 Vilnius, Lithuania; saulius.pakalka@vilniustech.lt (S.P.); kestutis.valancius@vilniustech.lt (K.V.)
[2] Applied Research Institute for Prospective Technologies, Vismaliuku str. 34, 10243 Vilnius, Lithuania
* Correspondence: giedre.streckiene@vilniustech.lt

Abstract: Latent heat thermal energy storage systems allow storing large amounts of energy in relatively small volumes. Phase change materials (PCMs) are used as a latent heat storage medium. However, low thermal conductivity of most PCMs results in long melting (charging) and solidification (discharging) processes. This study focuses on the PCM melting process in a fin-and-tube type copper heat exchanger. The aim of this study is to define analytically natural convection heat transfer coefficient and compare the results with experimental data. The study shows how the local heat transfer coefficient changes in different areas of the heat exchanger and how it is affected by the choice of characteristic length and boundary conditions. It has been determined that applying the calculation method of the natural convection occurring in the channel leads to results that are closer to the experiment. Using this method, the average values of the heat transfer coefficient (h_{ave}) during the entire charging process was obtained 68 W/m^{2}K, compared to the experimental result h_{ave} = 61 W/m^{2}K. This is beneficial in the predesign stage of PCM-based thermal energy storage units.

Keywords: phase change material (PCM); heat transfer coefficient; natural convection; melting; fin-and-tube; heat exchanger

Citation: Pakalka, S.; Valančius, K.; Streckienė, G. Experimental and Theoretical Investigation of the Natural Convection Heat Transfer Coefficient in Phase Change Material (PCM) Based Fin-and-Tube Heat Exchanger. *Energies* **2021**, *14*, 716. https://doi.org/10.3390/en14030716

Academic Editor: Ioan Sarbu
Received: 24 December 2020
Accepted: 27 January 2021
Published: 30 January 2021

1. Introduction

Efficient use of renewable energy sources is usually linked to the practical ability to accumulate energy. One of the main energy forms used in industrial and residential applications is heat. The overview of heat storage methods is presented in [1]. The comparison of sensible heat storage technology with latent heat storage (LHS) shows that the latter method has greater storage density, which allows to reduce the volume of the storage system. Therefore, LHS systems that use phase change materials (PCMs) are defined as an efficient method of storing heat. The comparison of the two storage technologies shows that systems with PCM have great design variety and many types of materials when specific thermophysical properties of PCM are concerned. Various PCMs and the areas of application thereof have been reviewed in [2,3].

Even though LHS systems with PCM have many technological advantages of heat accumulation when compared to sensible heat storage systems, one of the critical parameters of such materials is thermal conductivity [4]. Various measures allow to intensify the heat transfer process, but in order for these systems to become mainstream in the commercial market, intense systematic research is still necessary [5,6]. To solve the issue of heat transfer, design solutions and techniques that enhance thermal conductivity are employed, such as nanoparticles [7], porous and low-density materials [4], microencapsulated PCMs, metal foams and graphite [8]. Combined solutions are also available. One of the main techniques for heat enhancement in LHS systems is the use of extended surfaces [9], e.g., fins [10] with

shell and tube heat exchangers being the most widely used for this purpose [11,12]. The use of such heat exchangers along with PCMs allows to achieve an energy efficiency of more than 70% [8]. The addition of fins can accelerate the melting process by almost 50% [13] which reduces the charging time, but also leads to the need to optimise the processes of manufacturing heat exchangers, taking the production costs into account [14,15], as well as the need to consider the critical geometric parameters of heat exchangers listed in [8].

Many researchers have analysed various types of fins, their configuration, forms, used materials, manufacturing method thereof as well as the influence of the geometry of the storage tank [16,17]. Various physical phenomena, such as natural convection, were also studied separately or together. Experimental research of the effects of natural convection during phase change process was carried out as early as 50 years ago [18], but the search of appropriate PCMs, the choice thereof for specific applications and the analysis of processes, continues. Hale Jr and Viskanta [19] carried out experimental studies of the phase change of paraffin. The studies were concerned with the importance of natural convection for heat transfer during PCM melting. Experimental research performed by Stritih showed that natural convection may be more than 10 times higher during the melting process than during the solidification process. Meanwhile, in the case of PCM solidification the dominating heat transfer method is conductivity [20,21]. Other studies and overviews confirm the importance of natural convection in the melting process [22,23] which causes the recirculation of the fluid [24] and more intense heat transfer [25]. It has been noticed that currents of natural convection, when properly activated, allow to reduce the charging time of the storage system. It is necessary to describe this process in numeric and analytic research [26]. For example, one experimental study [27] showed that natural convection reduced the phase change time (solid to liquid) by 45% during heat transfer from vertical surfaces; another experimental study [28] showed that the melting time was reduced from 18.8% to 50.8%, depending on the varying conditions.

The processes of PCM melting and solidification in a finned vertical wall, considering the length of the fin, under the influence of the dominating natural convection effect were analysed numerically by Lacroix and Benmadda [29]. The influence of the temperature of heat transfer fluid inlet and mass flow rate on these phase-change processes were studied experimentally by Akgün et al. in [24]. Hosseini et al. [30,31] numerically and experimentally analysed the development of the PCM (RT50) melting process in a shell and tube heat exchanger. Their study suggested a correlation between the dynamic viscosity of the PCM and the temperature. The asymmetry of the melting process due to natural convection in a horizontal shell and tube LHS system has been described by Avci and Yazici [25]. This tendency was also noticed by Seddegh et al. [32], who later in [33] presented insights about natural convection in a vertical shell and tube LHS system. Vogel et al. [34] performed a numerical study and introduced a new non-dimensional indicator—the convective enhancement factor for assessing the effect of natural convection. The authors have also indicated the need of additional studies related to a deeper understanding of the heat transfer mechanism. Joybari et al. [35] studied the natural convection phenomenon by using the front tracking method. They separated the upper and lower areas of the system in a horizontal heat exchanger due to buoyancy forces that affect these areas differently. Han et al. [12] analysed the effect of natural convection on the operation of a LHS system with different areas of heat transfer fluid (HTF) inlet points. The results showed that natural convection is negligible when HTF input occurs in the upper area and leads to an inconsistent distribution of solid-liquid phase in various directions of the heat exchanger (HX). Deng et al. [26] numerically analysed the influence of shell conductivity, fin length and heat transfer fluid temperature parameters on the melting of the PCM in a horizontal shell and tube HX. The effect of natural convection was also assessed and was shown to be different in various areas of the HX. Experimental studies carried out by Mehta et al. [36] also confirmed that in the case of a shell and tube HX with a horizontal configuration, melting starts earlier in the upper area due to the phenomenon of natural convection. Mahdi et al. [13] analysed the development of the melting process (charging) of paraffin

wax in a shell and tube LHS unit and determined that the process was more efficient when the system orientation was horizontal. The presented studies show that the understanding, description and assesment of natural convection is necessary when analysing LHS systems and should be integrated when planning and designing such systems.

In order to discover a convenient and adequately accurate design method or tool for LHS systems, researchers study these systems analytically or semi-analytically [37]. To simplify the problems analysed, the physical properties of PCMs are often considered to be stable [16] and the material itself, during the phase-change, remains homogenous [12], the flow regime of the PCM is laminar [32]. Lamberg [38] has suggested a simplified analytical model which allowed to estimate the solid-liquid interface location and analyse the temperature distribution in the fin. However, the accuracy of the suggested model was strongly influenced by the geometry of storage. Mosaffa et al. [16] presented an analytical solution of the solidification process of the PCM in a shell and tube HX. Bechiri and Mansouri [39] analytically studied the performance of a shell and tube LHS system using the variable separation technique and the exponential integral function. The effect of natural convection was evaluated by the effective thermal conductivity. Mazzeo et al. [40] presented an exact analytical solution for solving the problem of steady periodic heat transfer in the PCM layer. Kalapala and Devanuri in their overview noted many factors to be taken into consideration during the design phase, e.g., the orientation of the HX, the number, width and length of the fin, while shell to tube diameter ratio was determined to be the most influential parameter [11]. A simplified model based on the enhanced thermal conductivity approach and the scaling theory for PCM melting with radiation and natural convection is presented by Souayfane et al. [22]. According to their results the natural convection effect enhanced heat transfer by 40 to 55% and increased the liquid fraction by about 35% compared to a conduction-only model. Fornarelli et al. [41] presented a simplified theoretical calculation model for a shell and tube HX, which could be used to estimate the melting time that could contribute to the designing phases of such systems by calculating their charging time. The results have shown the need of appropriate correlative equations for Nu–Re criteria when geometric modifications of the system are present. Many authors note that more comprehensive studies of heat transfer in systems with PCMs [42] and detailed theoretical models for fin based enhancement in LHS [37,43] are needed. There is also a noticeable lack of studies when the primary assessment of thermophysical properties of PCM in analytical calculations, numerical models and design works is analysed separately. A more accurate assessment of PCMs could allow to reduce failures of the designed LHS systems [44].

The analysis of convective heat transfer due to natural convection also poses another discussion subject—the choice of characteristic length [34,42]. In order to contribute to a better understanding of natural convection process in shell and fin-and-tube HXs with PCM and practical design of LHS systems, we have carried out analytical calculations and experimental tests by expressing the heat transfer coefficient. The objective of the study is to present calculation methods that allow to determine the heat transfer coefficient for a PCM-based horizontal shell and fin-and-tube HX system as accurately as possible. Our results further enable faster estimation of natural convection in LHS systems with a similar configuration without expensive and time-consuming analysis. Thus, the design of LHS systems could be cheaper, faster and facilitated.

2. Experimental Setup

The experimental study was carried out using an experimental setup (see Figure 1) made specifically for testing PCM-based thermal energy storage (TES) systems. This experimental setup was also used and described in detail in previous studies [6,45,46].

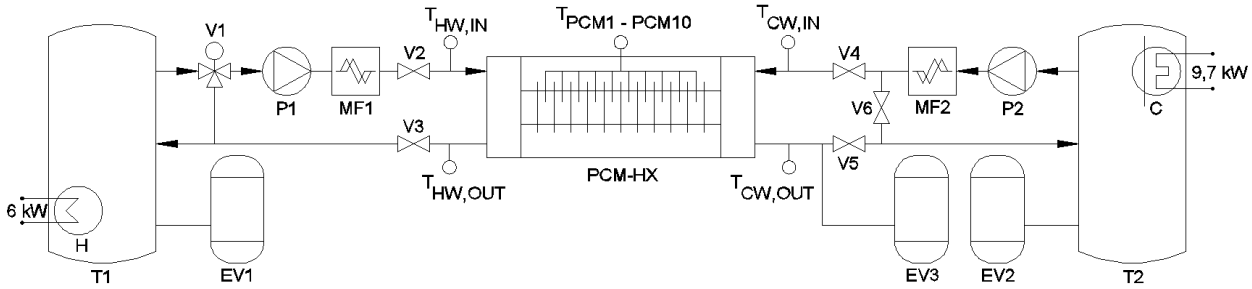

Figure 1. Schematic representation of the experimental setup (T_{PCM}, T_{HW} and T_{CW}—temperature sensors; T1, T2—tanks for hot and cold water storage; EV1, EV2, EV3—expansion vessels; H—hot water heater, C—cold water cooler; V1—mixing valve with electronic constant temperature controller; V2–V6—manual valves; MF1, MF2—flowmeters; P1, P2—circulating pumps).

The subject of the study is a PCM-based TES unit with a copper heat exchanger (PCM-HX) (Figures 2 and 3). This unit consists of a stainless-steel storage tank that has a copper HX installed inside of it (fin-and-tube type). External arrangement of PCM was selected—the storage tank volume has been filled with organic PCM RT82 (see Figure 3). This PCM-HX is designed to be used in industrial waste heat recovery/storage systems within the temperature range 90–100 °C, e.g., heat recovery from waste steam and condensate in autoclave and preheating of feed water. The analysed PCM-HX and PCM parameters are presented in Tables 1 and 2.

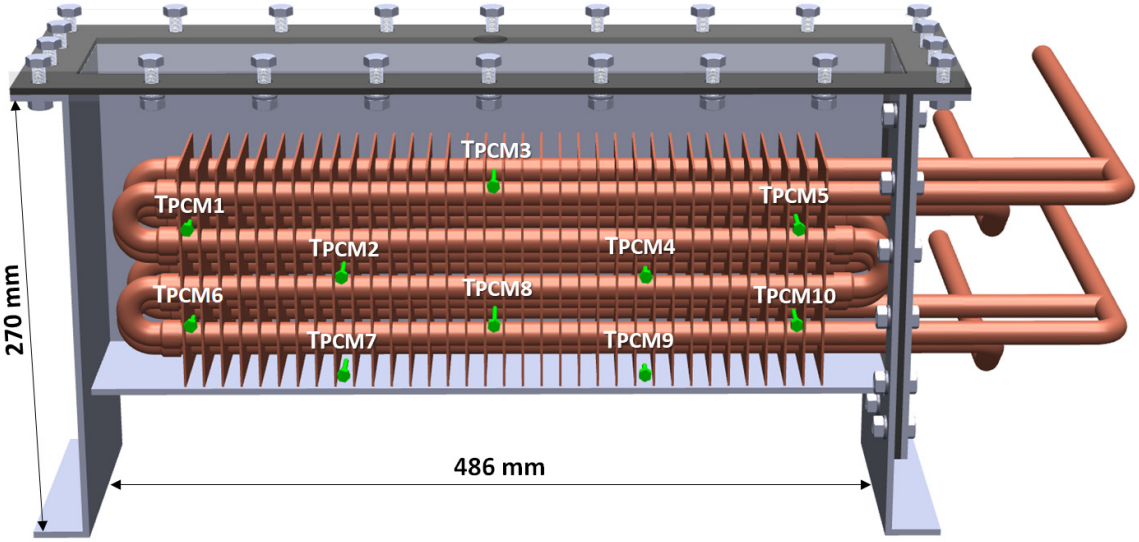

Figure 2. Positions of the temperature sensors.

Table 1. Parameters of analyzed PCM TES.

Fin quantity, units	35
Fin spacing, mm	10
Fin thickness, mm	1.5
Tube diameter (OD), mm	15
Tube thickness, mm	1.5
HX weight, kg	6.9
HX heat transfer area, m^2	0.89
PCM weight, kg	4.34
Heat transfer fluid (HTF)	Water

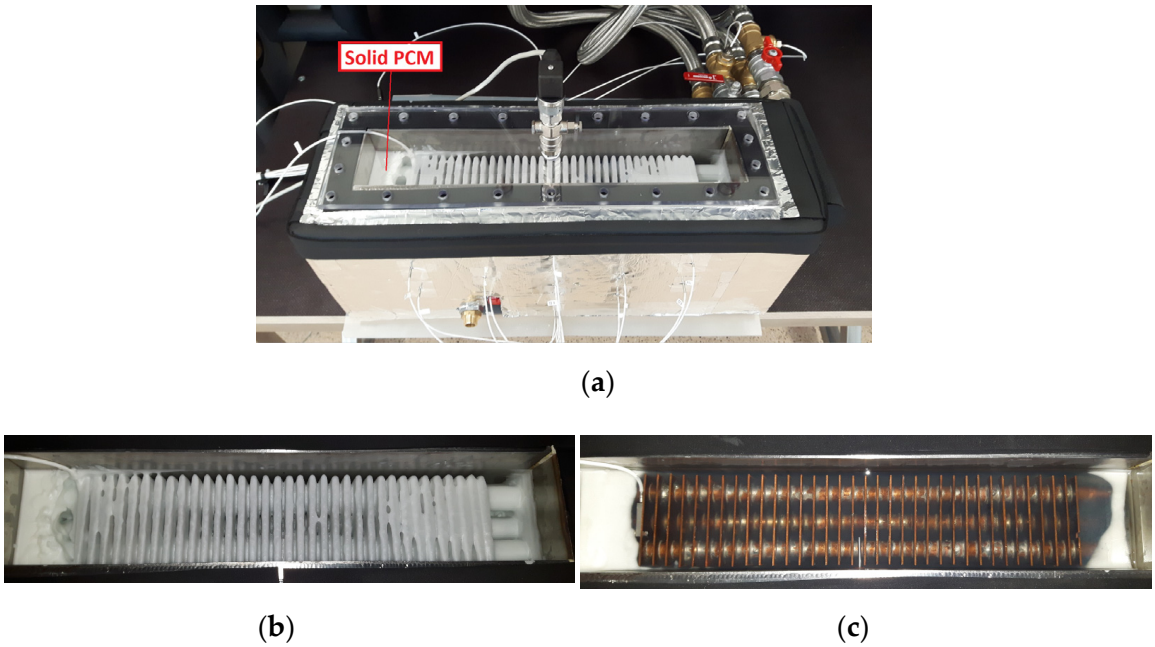

Figure 3. PCM-based TES unit with a copper heat exchanger (PCM-HX): (**a**) general view (**b**) the interior of the PCM-HX (the beginning of the melting process—solid PCM), (**c**) the interior of the PCM-HX (the end of the melting process—liquid PCM).

Table 2. Properties of PCM RT82.

Property	RT82
Melting area, °C	77–82
Congealing area, °C	82–77
Heat storage capacity (±7.5 %), kJ/kg	170
Specific heat capacity at constant pressure, kJ/kg K	2
Density solid at 15 °C, kg/L	0.88
Density liquid at 90 °C, kg/L	0.77
Heat conductivity (both phases), W/mK	0.2
Thermal expansion coefficient, 1/K [47,48]	0.001
Dynamic viscosity, kg/ms [47,48]	0.03499
Volume expansion, %	12.5

The experiment of charging the PCM (the melting process) is carried out in the experimental setup. At the beginning of the experiment, when the PCM is solid (see Figure 3b), with a temperature of 24 °C, inlet/outlet valves V2 and V3 of hot HTF are opened and hot HTF circulates through the copper HX and heat transfer with the PCM starts. During this experiment, the mass flow rate of the hot HTF is 0.4 kg/s, the temperature of the inlet HTF ($T_{HW, IN}$) is 94 ± 1 °C. Once the charging (melting) process ends (see Figure 3c), the PCM is cooled until it reaches the set temperature by using cold water from tank T2 in order to achieve the same starting conditions before another melting process begins. The cooling process is not analyzed in this study.

The temperature of PCM (T_{PCM1}–T_{PCM10}), hot water inlet ($T_{HW, IN}$) and outlet ($T_{HW, OUT}$) was measured with PT100 temperature sensors (see Figure 1, Figure 2, and Figure 4). The mass flow rate was measured with a calibrated Coriolis flow meter.

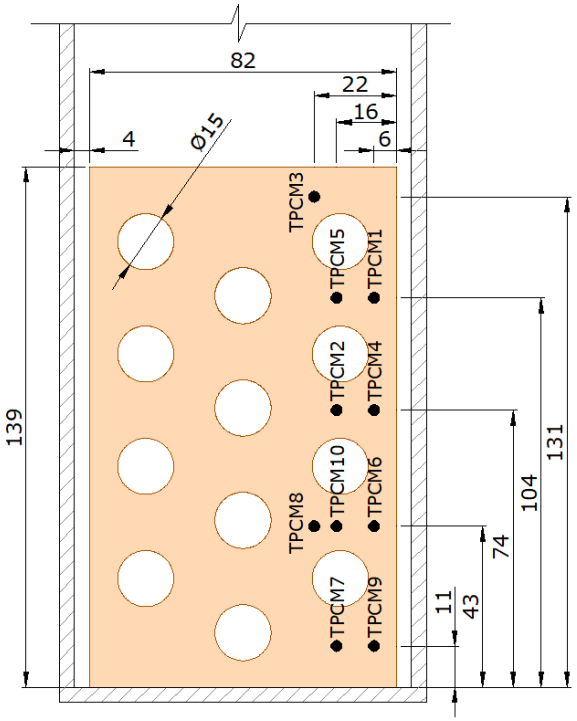

Figure 4. Positions of the temperature measuring points in the cross-section of the HX.

The positions of temperature sensors in the cross-section of HX are depicted in Figure 4. It should be noted that the positions of temperature measurement points are depicted in a single cross-section although there are five such cross-sections in the HX.

Reliability and repeatability: The experiment was repeated three times under the same operating and boundary conditions to ensure repeatability of results. The maximum standard deviation of inlet fluid is 2.0 °C at 94 °C during PCM charging (melting) process. Data logging interval is 5 Hz. The accuracy of the Coriolis mass flow meter is ±0.15%, temperature sensors Pt100, class B, accuracy ±(0.3 + 0.005 × t) °C. Temperature sensors have been accurately positioned and installed in the shell of the heat exchanger, thus the deformations occurring during the melting and solidification of the PCM do not affect the position of the sensor. The sensors have been installed in the shell by using compression fittings and the stainless-steel sheath of the temperature sensor has been separated from the shell wall with a Teflon (PTFE) ferrule, so heat conduction is negligible.

3. Theoretical Approach to Evaluate Natural Convection Heat Transfer Coefficient in PCM

The heat transfer rate ($\dot{Q}$) between the HTF (water) and the PCM was obtained by the following energy balance equation:

$$\dot{Q} = mc_p dT, \tag{1}$$

where m is the mass flow rate of the heat transfer fluid, kg/s; c_p is specific heat capacity at constant pressure, J/kgK; dT is the temperature difference, K.

The local heat transfer coefficient can be obtained from:

$$h_{PCM} = \frac{\dot{Q}}{A_{PCM}(T_{HX} - T_{PCM})}, \tag{2}$$

where h_{PCM} is PCM side heat transfer coefficient, W/m^{2}K; T_{HX} is the temperature of the HX (fins), K; A_{PCM} is the total heat transfer surface area to the PCM (fins and pipes), m^2; T_{PCM} is the temperature of the liquid PCM, K.

The temperature of the *HX* is calculated based on the average temperature of heat transfer fluid (water):

$$T_{HX} = \frac{(T_{HW,IN} + T_{HW,OUT})}{2}, \quad (3)$$

where $T_{HW,IN}$ is the temperature of the inlet HTF, K; $T_{HW,OUT}$ is the temperature of the outlet HTF, K.

On the basis of the literature overview it has been determined that the accuracy of the results of natural convection calculations depends on the adequate choice of the characteristic length. The choice of the characteristic length depends on the geometry of the HX, therefore, two cases of calculations (two different characteristic lengths) have been used in this study. The aim is to determine the results of which calculation method are closer to the results of the experiment on the HX configuration analyzed in this study. In the first case it is assumed that the heat transfer occurs from individual vertical plates (fins) and the characteristic length is the height of the vertical fin (L = 0.139 m). In the second case it is assumed that the heat transfer occurs between two fins that form a channel and then the characteristic length is the distance between two vertical fins (S = 0.01 m).

It should be noted that a simplified calculation method is used in this paper where it is assumed that the fins are isothermal (T_{HX} = constant) and fin efficiency $\eta_{fin} = 1$. Also, the calculations of the theoretical values of h do not consider the influence of the horizontal tubes (perpendicular to the fins) on the convective flows.

The calculation of the theoretical PCM side heat transfer coefficient when the characteristic length is the height of the vertical fin (L = 0.139 m) for the first case is presented below. The following equation to determine Rayleigh number is used:

$$Ra_L = \frac{g\beta(T_{HX} - T_{PCM})L^3}{v^2}\mathrm{Pr}, \quad (4)$$

where g is gravitational acceleration, m/s^2; β is PCM thermal expansion coefficient, 1/K; Pr is the Prandtl number, Pr = v/α; v is the kinematic viscosity of the fluid, m^2/s, $v = \mu/\rho$. The dynamic viscosity (μ) in the liquid PCM was considered to not be temperature dependent. α is the thermal diffusivity of the fluid, m^2/s, $\alpha = k/(\rho c_p)$; L is the characteristic length of the geometry (height of vertical fin), m; ρ is the density of the fluid, kg/m^3; k is the material thermal conductivity, W/(mK).

Nusselt number for the entire range of Ra is given by [49]:

$$\mathrm{Nu} = \left\{ 0.825 + \frac{0.387 Ra_L^{1/6}}{\left[1 + \left(\frac{0.492}{\mathrm{Pr}}\right)^{9/16}\right]^{8/27}} \right\}^2, \quad (5)$$

Once the Nu number is determined, the heat transfer coefficient (h) is calculated:

$$h_L = \frac{k}{L}\mathrm{Nu}, \quad (6)$$

The Rayleigh number for the second calculation case when the characteristic length is the distance between two vertical fins (the channel between two fins) is defined as:

$$Ra_S = \frac{g\beta(T_{HX} - T_{PCM})S^3}{v^2}\mathrm{Pr}, \quad (7)$$

where S is the characteristic length of the geometry (distance between to vertical fins), m.

Nusselt number when fins are isothermal (T_{HX} = constant) is calculated by [50]:

$$\mathrm{Nu} = \left[\frac{576}{\left(\frac{Ra_S S}{L}\right)^2} + \frac{2.873}{\left(\frac{Ra_S S}{L}\right)^{0.5}} \right]^{-0.5}, \quad (8)$$

Then the heat transfer coefficient is determined in accordance with another characteristic length:

$$h_S = \frac{k}{S}\mathrm{Nu}, \quad (9)$$

PCM density can be expressed as [51,52]:

$$\rho = \frac{\rho_L}{\beta(T - T_l) + 1}, \quad (10)$$

where T is the temperature of PCM, K; k is the thermal conductivity of PCM, W/mK; ρ is the density of PCM; ρ_l is the density of liquid PCM; T_1 is the temperature of liquid PCM, K.

4. Experimental and Theoretical Results and Discussion

The change of the experimentally obtained local heat transfer coefficients (h) and PCM temperatures (T) in different measurement points during the PCM charging (melting) process is shown in Figure 5. When the temperature reaches 77 °C in the respective measurement point, it is considered that the PCM begins to melt, so the values of h are only depicted when the liquid phase is present. In this case, as shown in the graph, in one of the measurements points the melting temperature is reached in 7.5 min from the beginning of the process (T_{PCM8}). In the point that is further away from the heat source the PCM begins to melt only after 40 min (T_{PCM1}).

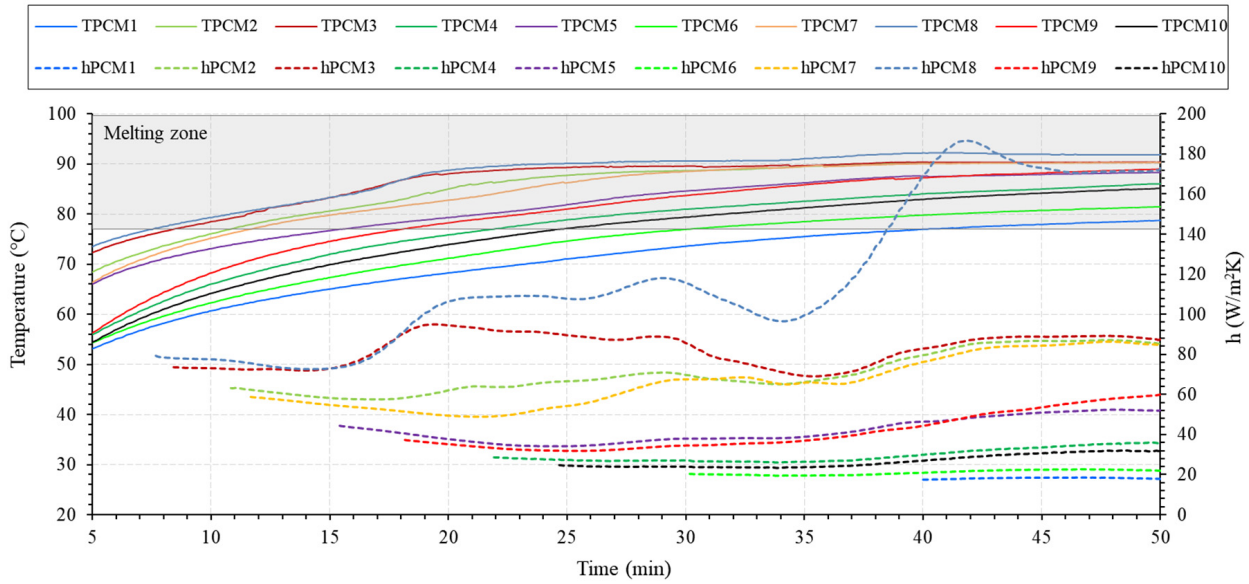

Figure 5. Variation of temperature and local heat transfer coefficient in different measurement points.

The graph (Figure 5) shows that the values of h in different measurement points decrease at the beginning of the melting process and from a certain point in time (depending on the location of measurement) start to increase. It should be noted that the increase of h occurs once the temperature exceeds 82 °C. This means that from the reference point (77 °C) phase change occurs in theory but is only at an early stage (a thin layer of liquid PCM), so natural convection has little influence on the heat transfer process. Once the temperature exceeds 82 °C, natural convection influences the heat transfer more because the PCM is

fully melted at the measurement point and convective currents are either formed or begin to form.

Once the temperature reaches 88 to 90 °C in measurement points T_{PCM2}, T_{PCM3}, T_{PCM7}, T_{PCM8}, the value of *h* decreases, which can be explained by a small drop of temperature of the HX (T_{HX}) within the interval from 25 to 35 min (Figures 6 and 7). Due to inertia in the aforementioned measurement points that are closer to the heat source the small decrease of the T_{HX} has greater influence on the value of local heat transfer coefficient compared to points further away from the heat source: h_{PCM1}, h_{PCM4}, h_{PCM5}, h_{PCM6}, h_{PCM9}, h_{PCM10}.

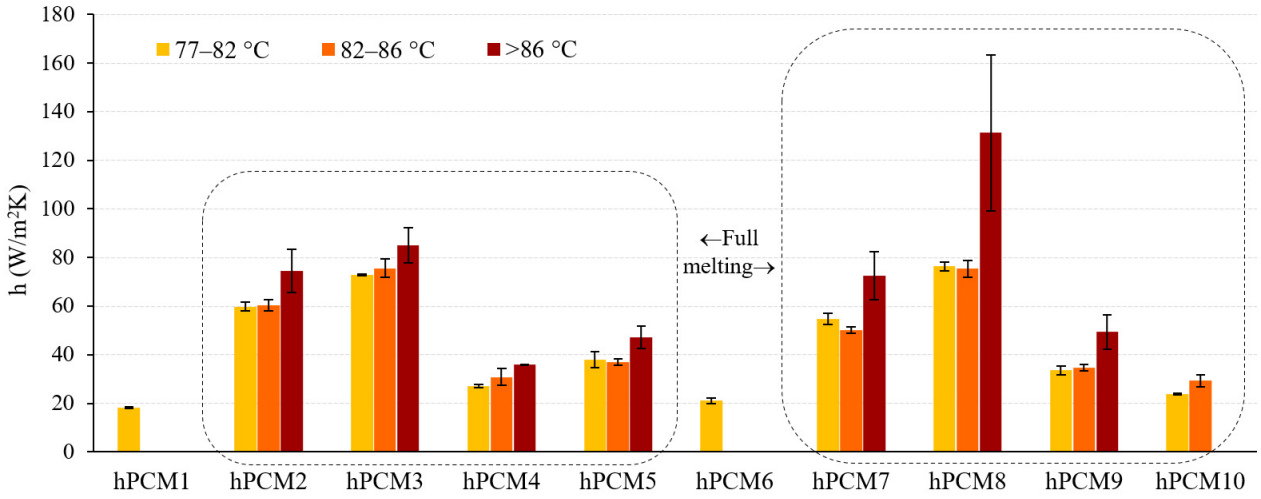

Figure 6. Variation of experimentally estimated heat transfer coefficients (incl. standard deviation).

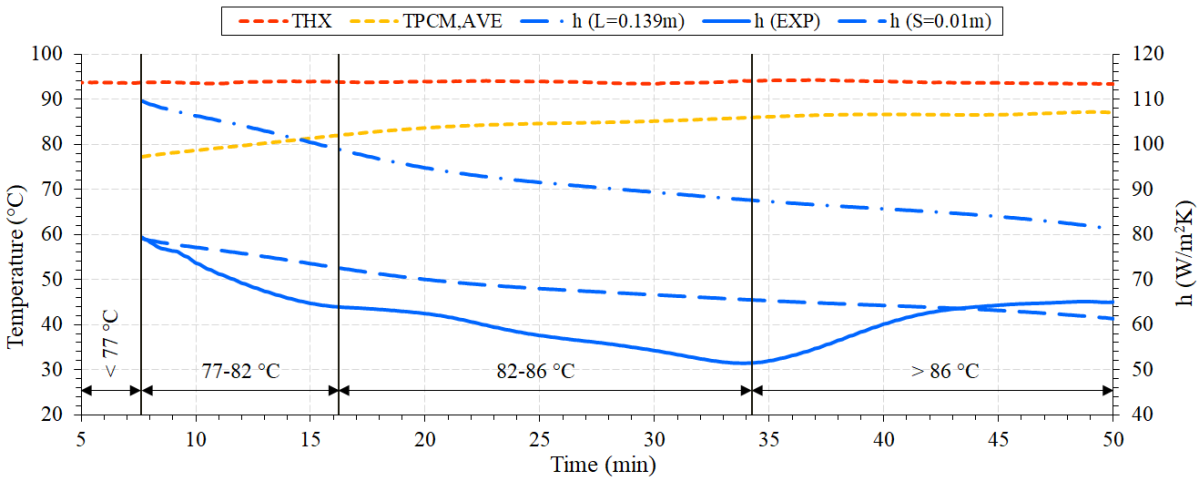

Figure 7. Average heat transfer coefficient: *h* (EXP)—experimental, *h* (*L* = 0.139 m)—theoretical (characteristic length fin height), *h* (S = 0.01 m)—theoretical (characteristic length fin spacing).

The graph (Figure 5) also shows that the value of h_{PCM8}, once the temperature exceeds 90 °C, starts rising more significantly compared to other measurement points. One of the possible reasons is lower dynamic viscosity of the PCM in that measurement point because the temperature of T_{PCM8} is the highest (maximum temperature reached in this point during the melting process is 92.2 °C) compared to other measurement points (max. temp. of T_{PCM2}, T_{PCM3}, T_{PCM7} is 90.3 °C, 90.4 °C, 90.3 °C, respectively). Another possible reason is that convective heat transfer is more intense in this point due to the position of the sensor, which is in an open vertical channel and surrounded by horizontal tubes from all sides (see Figures 2 and 4). Thus, it is concluded that flow is thermally developing in this region. Convective currents from the horizontal tubes intensify the heat transfer in

the vertical direction. In comparison, h_{PCM3} which is located in the same vertical plane as h_{PCM8} also indicates higher values of h, but the sensor is not surrounded by horizontal tubes and is in the upper layer, so it is likely that there is a fully thermally developed flow in this point.

Since the range of variation in experimental values of h is rather wide and depends on the temperature of the PCM and the position of the measurement point, average values of h at certain intervals should be determined. In this case, three temperature intervals were (Figure 6): 77–82 °C—theoretical interval of the PCM phase transition, 82–86 °C—liquid phase, >86 °C—the increase of the value of h is observed in the liquid phase (see Figure 5).

Figure 6 shows that within the intervals of 77 to 82 °C and 82 to 86 °C, the difference of average values of h fluctuates from 1 % (h_{PCM2}) to 22 % (h_{PCM10}). Within the temperature interval above 86 °C a higher h is noticed in all measurement points, except those where the temperature does not reach the value of this interval (h_{PCM1}, h_{PCM6}, h_{PCM10}). Therefore, when analysing the average values of h at the selected temperature intervals, the same tendency as for local h (Figure 5), is noticed, i.e., once the melting temperature of the PCM exceeds 4 °C, the value of h increases, which is linked to the decreasing dynamic viscosity of the material. It should be noted that the position of the sensor also influences the value of h.

In order to compare how experimental data correlates with the theoretical calculations of h, Figure 7 depicts the curves of the variation in the average value of h.

T_{HX} is the average temperature of the HX during the melting process of the PCM. $T_{PCM,AVE}$ depicts the average temperature of the PCM in the liquid phase, calculated using the readings of all temperature sensors that are in the liquid phase.

Figure 7 shows that characteristic length significantly affects the theoretical value of the heat transfer coefficient. If the distance between two fins is selected as the characteristic length, the theoretical curve is close to the experimental one (h (EXP)). When the height of the fin is the characteristic length, the values of h (L = 0.139 m) are higher when compared to h (S = 0.01 m) and h (EXP). The temperature profiles of both theoretical cases are similar, and the same tendency is observed once the average temperature of the PCM reaches 82 °C, i.e., the slope of curves decreases. The change of the experimental value fluctuates during the entire process and, once the average temperature of the PCM reaches 86 °C, the value of h (EXP) increases. When calculating the theoretical values of h, dynamic viscosity in the liquid PCM was considered to not be temperature-dependent, but as the temperature actually increases, the dynamic viscosity of the PCM decreases. Lower dynamic viscosity results in a more efficient convection.

It should be noted that Figure 7 shows average values of the heat transfer coefficient based on the average temperature of the PCM and does not show h variation in different positions in the HX. In order to evaluate the average values in more detail and compare with the experiment, different temperature intervals are analysed (Figure 8).

Figure 8 shows that once the temperature exceeds 86 °C, the average values of h_{ave}(S = 0.01 m) and h_{ave}(EXP) are very similar, 63.6 W/m^{2}K and 60.8 W/m^{2}K, respectively. The average values of h_{ave} during the entire charging process are: h_{ave}(EXP)—61 W/m^{2}K; h_{ave}(L = 0.139 m)—92 W/m^{2}K; h_{ave} (S = 0.01 m)—68 W/m^{2}K. Therefore, calculating in the case of the channel between two fins, the resulting average value of h is 7 W/m^{2}K higher than the experimental value on average and in the case of the vertical fin, the resulting average value of h is 31 W/m^{2}K higher than the experimental value. This shows that for HXs of this type, when assessing heat transfer occurring due to natural convection, the calculation method for the convection occurring in the channel may be applied. However, the proportions of the HX should be taken into consideration, because the ratio of fin height to channel width also affects the influence of convection on the heat transfer process. In addition to this, in this study the calculations of the theoretical value of h did not consider the horizontal tubes of the HX that in a way divide the HX into smaller areas (channels). It is difficult to calculate convective in these areas, because in one case the tubes may block the vertical convective current that occurs from the vertical surfaces (fins) and intensify it

in other cases. For example, in the regions of the HX that do not have restrictions in the vertical direction (see Figure 4) it is likely that we will have a fully developed channel flow. In areas closer to the tubes it is very likely that we will have a developing flow.

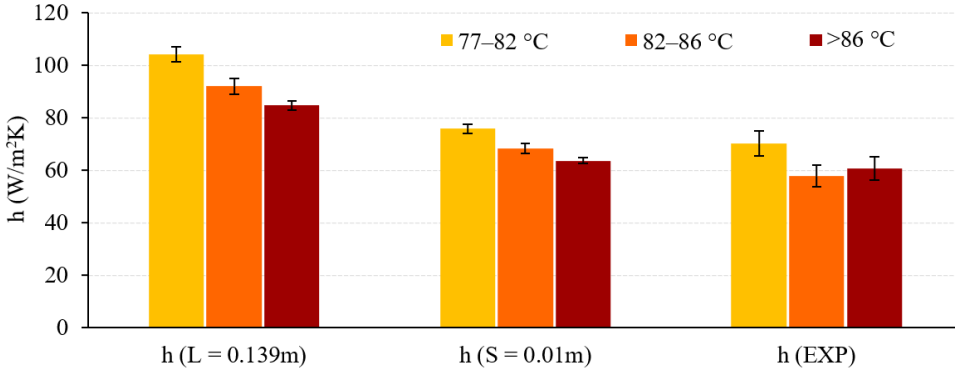

Figure 8. Comparison of average heat transfer coefficient (incl. standard deviation).

5. Conclusions

In the present study, an experimental and theoretical investigation was carried out to evaluate natural convection heat transfer coefficient. Literature review has demonstrated that there is a lack of studies that focus on the effect of natural convection on the PCM during the melting process and experimental results are compared to theoretical results. The adaptation of the analytical expression of natural convection to determining the PCM heat transfer coefficient allows to perform a primary assessment of separate thermophysical and design parameters. Results of experimental studies identify the values of local heat transfer coefficient in different areas of the HX while the comparison of the theoretical and experimental values of h during the entire melting process and/or at different intervals provides practical benefits when designing such systems.

The study on shell and tube-and-fin type of TES has shown that the theoretical results are closer to the experimental results when the selected characteristic length is the distance between two vertical fins (the channel between two fins). If the fin height is selected as the characteristic length, higher values of h_{ave} are seen, which during the entire charging process are: h_{ave}(EXP)—61 W/m^{2}K; h_{ave}(L = 0.139 m)—92 W/m^{2}K; h_{ave}(S = 0.01 m)—68 W/m^{2}K. During the experimental study, it has been noticed that convective heat transfer also occurs from the surface of the tubes and it is likely that in certain points convective currents from vertical and horizontal surfaces intensify each other and in certain points restrict the formation of convective currents in the vertical direction.

It has been determined that the average value of h increases once the temperature exceeds 86 °C during the experiment, which contradicts theoretical calculations. It is assumed that this difference is influenced by the dynamic viscosity of the PCM which increases with the increase of temperature and intensifies the natural convection. In theoretical calculations it is assumed that dynamic viscosity is constant, so the increase of the value of h was not noticed. In order to assess the influence of dynamic viscosity on the process of heat transfer more accurately, the dependence of the dynamic viscosity of the PCM on the temperature should be determined.

Author Contributions: Conceptualization, S.P. and K.V.; methodology, S.P.; validation, S.P. and K.V.; formal analysis, G.S.; investigation, S.P. and K.V.; resources, G.S. and S.P.; data curation, G.S.; writing—original draft preparation, S.P. and G.S.; writing—review and editing, K.V. and G.S.; visualization, S.P.; supervision, K.V. All authors have read and agreed to the published version of the manuscript.

Funding: This research received no external funding.

Institutional Review Board Statement: Not applicable.

Informed Consent Statement: Not applicable.

Data Availability Statement: The data presented in this study are available on request from the corresponding author.

Conflicts of Interest: The authors declare no conflict of interest.

Nomenclature

Latin letters	
A_{PCM}	total heat transfer surface area to the PCM (fins and pipes) [m^2]
c_p	specific heat capacity at constant pressure [J/kgK]
g	gravitational acceleration [m/s^2]
h	heat transfer coefficient [W/m^2K]
k	thermal conductivity [W/mK]
L	characteristic length of the geometry (height of vertical fin) [m]
m	mass flow rate [kg/s]
Nu	Nusselt number [–]
Pr	Prandtl number [–]
$\dot{Q}$	heat transfer rate [W]
Ra	Rayleigh number [–]
S	characteristic length of the geometry (distance between two vertical fins) [m]
T	Temperature [K], [°C]
Greek	
α	thermal diffusivity [m^2/s]
β	thermal expansion coefficient [1/K]
η_{fin}	fin efficiency
μ	dynamic viscosity [Pa·s]
ρ	density [kg/m^3]
v	kinematic viscosity [m^2/s]
Subscripts	
1, 2, ...	position No
AVE	average
CW	cold water
HW	hot water
HX	heat exchanger
IN	inlet
L	height of vertical fin
l	liquid
OUT	outlet
PCM	phase change material
S	distance between to vertical fins
Abbreviations	
C	cold water cooler
EV	expansion vessel
EXP	experimental
H	hot water heater
HTF	heat transfer fluid
HX	heat exchanger
LHS	latent heat storage
MF	flowmeter
P	circulating pump
PCM	phase change material
PCM-HX	phase change material-based heat exchanger
T	temperature sensor or tank for water storage
TES	thermal energy storage
V	valve

References

1. Sarbu, I.; Sebarchievici, C. A Comprehensive Review of Thermal Energy Storage. *Sustainability* **2018**, *10*, 191. [CrossRef]
2. Da Cunha, J.P.; Eames, P.C. Thermal Energy Storage for Low and Medium Temperature Applications Using Phase Change Materials—A Review. *Appl. Energy* **2016**, *177*, 227–238. [CrossRef]
3. Ali, S.; Deshmukh, S. An Overview: Applications of Thermal Energy Storage Using Phase Change Materials. *Mater. Today: Proc.* **2020**, *26*, 1231–1237. [CrossRef]
4. Liu, L.; Su, D.; Tang, Y.; Fang, G. Thermal Conductivity Enhancement of Phase Change Materials for Thermal Energy Storage: A Review. *Renew. Sustain. Energy Rev.* **2016**, *62*, 305–317. [CrossRef]
5. Wu, S.; Yan, T.; Kuai, Z.; Pan, W.-G. Thermal Conductivity Enhancement on Phase Change Materials for Thermal Energy Storage: A Review. *Energy Storage Mater.* **2020**, *25*, 251–295. [CrossRef]
6. Pakalka, S.; Valančius, K.; Streckienė, G. Experimental Comparison of the Operation of PCM-Based Copper Heat Exchangers with Different Configurations. *Appl. Therm. Eng.* **2020**, *172*, 115138. [CrossRef]
7. Nitsas, M.; Koronaki, I.P. Thermal Analysis of Pure and Nanoparticle-Enhanced PCM—Application in Concentric Tube Heat Exchanger. *Energies* **2020**, *13*, 3841. [CrossRef]
8. Zayed, M.E.; Zhao, J.; Li, W.; Elsheikh, A.H.; Elbanna, A.M.; Jing, L.; Geweda, A. Recent Progress in Phase Change Materials Storage Containers: Geometries, Design Considerations and Heat Transfer Improvement Methods. *J. Energy Storage* **2020**, *30*, 101341. [CrossRef]
9. Ibrahim, N.I.; Al-Sulaiman, F.A.; Rahman, S.; Yilbas, B.S.; Sahin, A.Z. Heat Transfer Enhancement of Phase Change Materials for Thermal Energy Storage Applications: A Critical Review. *Renew. Sustain. Energy Rev.* **2017**, *74*, 26–50. [CrossRef]
10. Zhang, S.; Pu, L.; Xu, L.; Liu, R.; Li, Y. Melting Performance Analysis of Phase Change Materials in Different Finned Thermal Energy Storage. *Appl. Therm. Eng.* **2020**, *176*, 115425. [CrossRef]
11. Kalapala, L.; Devanuri, J.K. Influence of Operational and Design Parameters on the Performance of a PCM Based Heat Exchanger for Ther-Mal Energy Storage—A Review. *J. Energy Storage* **2018**, *20*, 497–519. [CrossRef]
12. Han, G.-S.; Ding, H.-S.; Huang, Y.; Tong, L.; Ding, Y. A Comparative Study on the Performances of Different Shell-and-Tube Type Latent Heat Thermal Energy Storage Units Including the Effects of Natural Convection. *Int. Commun. Heat Mass Transf.* **2017**, *88*, 228–235. [CrossRef]
13. Mahdi, M.S.; Hasan, A.F.; Mahood, H.B.; Campbell, A.N.; Khadom, A.A.; Karim, A.M.A.; Sharif, A.O. Numerical Study and Experimental Validation of the Effects of Orientation and Configuration on Melting in a Latent Heat Thermal Storage Unit. *J. Energy Storage* **2019**, *23*, 456–468. [CrossRef]
14. Hosseini, M.; Ranjbar, A.; Rahimi, M.; Bahrampoury, R. Experimental and Numerical Evaluation of Longitudinally Finned Latent Heat Thermal Storage Systems. *Energy Build.* **2015**, *99*, 263–272. [CrossRef]
15. Pakalka, S.; Valančius, K.; Čiuprinskas, K.; Pum, D.; Hinteregger, M. Analysis of Possibilities to Use Phase Change Materials in Heat Exchangers-Accumulators. In Proceedings of the 10th International Conference "Environmental Engineering", Vilnius Gediminas Technical University, Vilnius, Lithuania, 27–28 April 2017.
16. Mosaffa, A.; Talati, F.; Tabrizi, H.B.; Rosen, M.A. Analytical Modeling of PCM Solidification in a Shell and Tube Finned Thermal Storage for Air Conditioning Systems. *Energy Build.* **2012**, *49*, 356–361. [CrossRef]
17. Castell, A.; Solé, C.; Medrano, M.; Roca, J.; Cabeza, L.F.; García, D. Natural Convection Heat Transfer Coefficients in Phase Change Material (PCM) Modules with External Vertical Fins. *Appl. Therm. Eng.* **2008**, *28*, 1676–1686. [CrossRef]
18. Szekely, J.; Chhabra, P.S. The Effect of Natural Convection on the Shape and Movement of the Melt-Solid Interface in the Controlled Solidification of Lead. *Met. Mater. Trans. A* **1970**, *1*, 1195–1203. [CrossRef]
19. Hale, N.; Viskanta, R. Photographic Observation of the Solid-Liquid Interface Motion during Melting of a Solid Heated from an Iso-Thermal Vertical Wall. *Lett. Heat Mass Transf.* **1978**, *5*, 329–337. [CrossRef]
20. Stritih, U. An Experimental Study of Enhanced Heat Transfer in Rectangular PCM Thermal Storage. *Int. J. Heat Mass Transf.* **2004**, *47*, 2841–2847. [CrossRef]
21. Fadl, M.; Eames, P. Thermal Performance Analysis of the Charging/Discharging Process of a Shell and Horizontally Oriented Multi-Tube Latent Heat Storage System. *Energies* **2020**, *13*, 6193. [CrossRef]
22. Souayfane, F.; Biwole, P.H.; Fardoun, F. Melting of a Phase Change Material in Presence of Natural Convection and Radiation: A Simplified Model. *Appl. Therm. Eng.* **2018**, *130*, 660–671. [CrossRef]
23. Gadgil, A.; Gobin, D. Analysis of Two-Dimensional Melting in Rectangular Enclosures in Presence of Convection. *J. Heat Transf.* **1984**, *106*, 20–26. [CrossRef]
24. Akgün, M.; Aydın, O.; Kaygusuz, K. Experimental Study on Melting/Solidification Characteristics of a Paraffin as PCM. *Energy Convers. Manag.* **2007**, *48*, 669–678. [CrossRef]
25. Avci, M.; Yazici, M.Y. Experimental Study of Thermal Energy Storage Characteristics of a Paraffin in a Horizontal Tube-in-Shell Storage Unit. *Energy Convers. Manag.* **2013**, *73*, 271–277. [CrossRef]
26. Deng, S.; Nie, C.; Wei, G.; Ye, W.-B. Improving the Melting Performance of a Horizontal Shell-Tube Latent-Heat Thermal Energy Storage Unit Using Local Enhanced Finned Tube. *Energy Build.* **2019**, *183*, 161–173. [CrossRef]
27. Sun, X.; Zhang, Q.; Medina, M.A.; Lee, K.O. Experimental Observations on the Heat Transfer Enhancement Caused by Natural Convection during Melting of Solid–Liquid Phase Change Materials (PCMs). *Appl. Energy* **2016**, *162*, 1453–1461. [CrossRef]

28. Sun, X.; Chu, Y.; Mo, Y.; Fan, S.; Liao, S. Experimental Investigations on the Heat Transfer of Melting Phase Change Material (PCM). *Energy Procedia* **2018**, *152*, 186–191. [CrossRef]
29. Lacroix, M.; Benmadda, M. Numerical Simulation of Natural Convection-Dominated Melting and Solidification from a Finned Vertical Wall. *Numer. Heat Transfer Part A Appl.* **1997**, *31*, 71–86. [CrossRef]
30. Hosseini, M.; Ranjbar, A.; Sedighi, K.; Rahimi, M. A Combined Experimental and Computational Study on the Melting Behavior of a Medium Temperature Phase Change Storage Material inside Shell and Tube Heat Exchanger. *Int. Commun. Heat Mass Transf.* **2012**, *39*, 1416–1424. [CrossRef]
31. Hosseini, M.; Rahimi, M.; Bahrampoury, R. Experimental and Computational Evolution of a Shell and Tube Heat Exchanger as a PCM Thermal Storage System. *Int. Commun. Heat Mass Transf.* **2014**, *50*, 128–136. [CrossRef]
32. Seddegh, S.; Wang, X.; Henderson, A.D. A Comparative Study of Thermal Behaviour of a Horizontal and Vertical Shell-and-Tube Energy Storage Using Phase Change Materials. *Appl. Therm. Eng.* **2016**, *93*, 348–358. [CrossRef]
33. Seddegh, S.; Joybari, M.M.; Wang, X.; Haghighat, F. Experimental and Numerical Characterization of Natural Convection in a Vertical Shell-and-Tube Latent Thermal Energy Storage System. *Sustain. Cities Soc.* **2017**, *35*, 13–24. [CrossRef]
34. Vogel, J.; Felbinger, J.; Johnson, M. Natural Convection in High Temperature Flat Plate Latent Heat Thermal Energy Storage Systems. *Appl. Energy* **2016**, *184*, 184–196. [CrossRef]
35. Joybari, M.M.; Haghighat, F.; Seddegh, S. Natural Convection Characterization during Melting of Phase Change Materials: Development of a Simplified Front Tracking Method. *Sol. Energy* **2017**, *158*, 711–720. [CrossRef]
36. Banerjee, J.; Solanki, K.; Rathod, M.K.; Banerjee, J. Thermal Performance of Shell and Tube Latent Heat Storage Unit: Comparative Assessment of Horizontal and Vertical Orientation. *J. Energy Storage* **2019**, *23*, 344–362. [CrossRef]
37. Mostafavi, A.; Parhizi, M.; Jain, A. Semi-Analytical Thermal Modeling of Transverse and Longitudinal Fins in a Cylindrical Phase Change Energy Storage System. *Int. J. Therm. Sci.* **2020**, *153*, 106352. [CrossRef]
38. Lamberg, P. Approximate Analytical Model for Two-Phase Solidification Problem in a Finned Phase-Change Material Storage. *Appl. Energy* **2004**, *77*, 131–152. [CrossRef]
39. Bechiri, M.; Mansouri, K. Analytical Solution of Heat Transfer in a Shell-and-Tube Latent Thermal Energy Storage System. *Renew. Energy* **2015**, *74*, 825–838. [CrossRef]
40. Mazzeo, D.; Oliveti, G.; De Gracia, A.; Coma, J.; Solé, A.; Cabeza, L.F. Experimental Validation of the Exact Analytical Solution to the Steady Periodic Heat Transfer Problem in a PCM Layer. *Energy* **2017**, *140*, 1131–1147. [CrossRef]
41. Fornarelli, F.; Camporeale, S.; Fortunato, B. Simplified Theoretical Model to Predict the Melting Time of a Shell-and-Tube LHTES. *Appl. Therm. Eng.* **2019**, *153*, 51–57. [CrossRef]
42. Vogel, J.; Johnson, M. Natural Convection during Melting in Vertical Finned Tube Latent Thermal Energy Storage Systems. *Appl. Energy* **2019**, *246*, 38–52. [CrossRef]
43. Mostafavi, A.; Parhizi, M.; Jain, A. Theoretical Modeling and Optimization of Fin-Based Enhancement of Heat Transfer into a Phase Change Material. *Int. J. Heat Mass Transf.* **2019**, *145*, 118698. [CrossRef]
44. Soni, V.; Kumar, A.; Jain, V.K. Modeling of PCM Melting: Analysis of Discrepancy between Numerical and Experimental Results and Energy Storage Performance. *Energy* **2018**, *150*, 190–204. [CrossRef]
45. Pakalka, S.; Valančius, K.; Damonskis, M. Effect of Open and Closed Operation Modes on the Performance of Phase Change Ma-Terial Based Copper Heat Exchanger. In Proceedings of the the 11th International Conference Environmental Engineering 11th Icee Selected Papers, Vilnius Gediminas Technical University, Vilnius, Lithuania, 21–22 May 2020; p. 2020611.
46. Pakalka, S.; Valančius, K.; Damonskis, M. Šilumnešio Debito Itakos Fazinio Virsmo Medžiagos Veikimui Tyrimas. *Moksl. Liet. Ateitis/Sci.—Futur. Lith.* **2018**, *10*, 1–6. [CrossRef]
47. Mat, S.; Al-Abidi, A.A.; Sopian, K.; Sulaiman, M.; Mohammad, A.T. Enhance Heat Transfer for PCM Melting in Triplex Tube with Internal–External Fins. *Energy Convers. Manag.* **2013**, *74*, 223–236. [CrossRef]
48. Mahdi, J.M.; Lohrasbi, S.; Ganji, D.D.; Nsofor, E.C. Simultaneous Energy Storage and Recovery in the TriplEx-tube Heat Exchanger with PCM, Copper Fins and Al2O3 Nanoparticles. *Energy Convers. Manag.* **2019**, *180*, 949–961. [CrossRef]
49. Churchill, S.W.; Chu, H.H. Correlating Equations for Laminar and Turbulent Free Convection from a Vertical Plate. *Int. J. Heat Mass Transf.* **1975**, *18*, 1323–1329. [CrossRef]
50. Bar-Cohen, A.; Rohsenow, W.M. Thermally Optimum Spacing of Vertical, Natural Convection Cooled, Parallel Plates. *J. Heat Transf.* **1984**, *106*, 116–123. [CrossRef]
51. Kandasamy, R.; Wang, X.-Q.; Mujumdar, A.S. Transient Cooling of Electronics Using Phase Change Material (PCM)-Based Heat Sinks. *Appl. Therm. Eng.* **2008**, *28*, 1047–1057. [CrossRef]
52. Xie, J.; Choo, K.F.; Xiang, J.; Lee, H.M. Characterization of Natural Convection in a PCM-Based Heat Sink with Novel Conductive Structures. *Int. Commun. Heat Mass Transf.* **2019**, *108*, 104306. [CrossRef]